

# Refractory Selection for High-Temperature Black Liquor Gasification

Alireza Rezaie,<sup>\*,†</sup> William L. Headrick,<sup>\*</sup> and William G. Fahrenholtz<sup>\*</sup>

Department of Ceramic Engineering, University of Missouri Rolla, Rolla, Missouri 65409

A methodology has been established for the selection of materials for refractory linings in black liquor gasifiers that are to be employed by the pulp and paper industry. As a first step, a thermodynamic software package was used to determine that black liquor smelt was composed of a liquid solution of primarily  $\text{Na}_2\text{CO}_3$  and  $\text{Na}_2\text{S}$  under the operating conditions of the gasifier ( $950^\circ\text{C}$ , 1 atm). Next, the software was used to predict the interaction of the black liquor smelt with various ceramics such as aluminosilicates, single component oxides, and binary oxides that are candidates for the application. Finally, experiments were performed to verify or disprove the predictions. Using sessile drop testing, contact angles were determined for molten  $\text{Na}_2\text{CO}_3$  on candidate refractory compounds. All of the candidate ceramics were wet by molten  $\text{Na}_2\text{CO}_3$ . Among the candidates,  $\text{MgAl}_2\text{O}_4$  was found to have the highest contact angle ( $\sim 13^\circ$ ). Post-mortem analysis was performed on sessile drop specimens using X-ray diffraction analysis and scanning electron microscopy with energy dispersive spectroscopy to determine if molten  $\text{Na}_2\text{CO}_3$  had penetrated into or reacted with the ceramics. From the candidates,  $\text{MgO}$  and  $\text{CeO}_2$  were found to have the best resistance to attack, while  $\text{MgAl}_2\text{O}_4$  was also found to be a promising candidate.

## I. Introduction

THE forest products industries, which include the papermaking industry, have been identified by the U.S. Department of Energy "Industries of the Future" and have been targeted for improvements in energy efficiency and reduction of waste streams.<sup>1</sup> The papermaking industry uses the kraft process to separate the cellulose fibers used to make paper from the other components of the wood (mainly lignin).<sup>2,3</sup> In the kraft process, a caustic solution of  $\text{NaOH}$  and  $\text{Na}_2\text{S}$  is employed to digest the lignin.<sup>2-4</sup> After separating the cellulose fibers, the resulting waste stream is a water solution containing lignin and the spent pulping chemicals, primarily  $\text{Na}_2\text{CO}_3$ , and  $\text{Na}_2\text{SO}_4$ .<sup>5</sup> Lignin, essentially a phenolic-type glue that holds wood together, contains a significant amount of chemical energy similar to other biomass-type fuels.<sup>6,7</sup> Sixty percent of the organic material in the original logs ends up in the black liquor.<sup>4</sup> Currently, the pulp and paper industry uses kraft recovery boilers to burn the black liquor and convert its chemical energy into high-pressure steam (40–100 atm), which can be used for generation of electricity or other purposes.<sup>8</sup> This energy is used to dry the pulp and paper, concentrate the black liquor, and power other equipment in the plant.<sup>9</sup> Although recovery boilers have been used successfully for many years, they have a number of shortcomings including

high capital expense, low efficiency, and the potential for explosion.<sup>5,10,11</sup>

Black liquor gasification is a moderate pressure ( $\sim 1$ – $3$  atm) steam reforming process.<sup>9,12</sup> Replacement of recovery boilers with gasification technology would improve energy efficiency, reduce hazardous emissions, and eliminate the potential for boiler explosions. Replacing the older boiler technology with gasifiers would improve the energy recovered from black liquor from the range of 500–800 kWh/ADMT<sup>‡</sup> for boilers to 1200–1800 kWh/ADMT for gasification, an increase in efficiency of 50% or more.<sup>12</sup> The increase in efficiency afforded by black liquor gasification as compared with the older recovery boiler technology could reduce or even eliminate the need for plants to purchase electricity for their operations.<sup>12,13</sup> Hence, black liquor gasification technology could enable one of the most energy intensive industries to become a net producer of electricity. Several distinct gasification technologies have been proposed, but only two have had satisfactory performance in plant trials.<sup>14</sup> One of the successful gasification technologies is a low-temperature steam reforming process ( $600^\circ$ – $700^\circ\text{C}$ ) while the other is a higher-temperature process ( $900^\circ$ – $1000^\circ\text{C}$ ) in which the black liquor is partially oxidized.<sup>15</sup> This paper focuses on refractory selection for the high-temperature gasification process, which is shown schematically in Fig. 1. The high-temperature process currently uses air for the partial combustion, however, conversion to oxy-fuel firing could potentially double the net power output from  $\sim 1200$  to  $\sim 2400$  kWh/ADMT.<sup>8</sup> In addition to increasing the overall process efficiency, oxygen enrichment of the combustion gas may increase the temperature inside the gasifier to as high as  $1400^\circ\text{C}$ , which could benefit chemical recovery because of lower  $\text{Na}_2\text{CO}_3$  levels in the smelt.<sup>8</sup>

The initial black liquor gasifier designs have incorporated low-cost materials such as aluminosilicates (e.g., common fire-clay brick) or more expensive fused-cast alumina refractories.<sup>4</sup> Plant trials and thermodynamic calculations both show that these materials are not sufficiently resistant to molten alkali compounds for extended operation of the gasifiers.<sup>4</sup> In general, the choice of refractory lining material must be a balance among expected lifetime, cost, and performance. Preliminary studies have focused, primarily, on understanding reactions that proceed during use.<sup>16–18</sup> This study will consider low-cost refractories (e.g., aluminosilicates), higher-cost commercial materials (e.g., magnesia, zirconia, alumina, and spinel), and novel materials (e.g., ceria, barium aluminate).

As a first step toward developing new refractories for black liquor gasifiers, a combination of thermodynamic modeling and interaction studies was conducted. The combined approach was used to identify potential interactions between black liquor smelt and candidate materials. Thermodynamic modeling was used to screen candidate materials. The second step was to test candidate materials to determine wetting characteristics and chemical interactions. Sessile drop testing was used because it allows for simultaneous evaluation of wetting behavior, physical penetration characteristics, and chemical interactions.<sup>19</sup>

The purpose of this paper is to describe a methodology that combines thermodynamic simulations with experimental

W. Lee—contributing editor

Manuscript No. 20057. Received January 21, 2005; approved July 27, 2005.

This report was prepared with the support of the U.S. Department of Energy, under Award No. DE-FC26-02NT41491. However, any opinions, findings, conclusions, or recommendations expressed herein are those of the authors and do not necessarily reflect the views of the DOE.

<sup>\*</sup>Member, American Ceramic Society.

<sup>†</sup>Author to whom correspondence should be addressed. e-mail: a\_rezaie76@hotmail.com

<sup>‡</sup>ADMT = Air Dried Metric Ton; kWh/ADMT is a measure of the energy recovered from 1 metric ton of pulp (1000 kg) with 10% residual moisture.

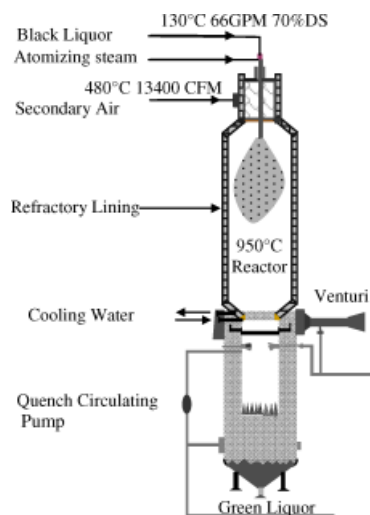


**Fig. 1.** Schematic diagram of a high-temperature, low-pressure black liquor gasifier based on descriptions provided in Keiser *et al.*<sup>5</sup> and Rezaie *et al.*<sup>16</sup>.

verification to screen potential refractory lining materials for black liquor gasifiers.

## II. Thermodynamic Simulations and Phase Diagram Analysis

Thermodynamic modeling was completed using a commercial software package (FactSage<sup>®</sup> 5.1, Thermfact Ltd., Montreal, Canada). The composition assumed for black liquor was based on typical compositions reported for North American softwoods and hardwoods (Table I).<sup>20</sup> The next step was to simulate the gasification process. It was assumed that the black liquor was combusted using a stoichiometric amount of oxygen at 950°C and a total pressure of 1 atm<sup>11,14</sup> so that free carbon was completely oxidized. Combustion is exothermic ( $\Delta H \approx -115$  kJ/mol for free C combusted to CO) because of the release of the chemical energy as the reaction products are formed. For the simulation, solution species were not considered, but all possible compounds were evaluated. Once the volatile combustion products were removed (primarily as CO, H<sub>2</sub>, and H<sub>2</sub>S),<sup>21</sup> the residual condensed phases that would be in contact with the refractory lining of the gasifier were referred to as black liquor smelt. The smelt consisted of mainly Na<sub>2</sub>CO<sub>3</sub> (~75 wt%) and Na<sub>2</sub>S (~25 wt%). At pressures above 2 atm, the software predicted the formation of a minor amount (<5 wt%) of K<sub>2</sub>CO<sub>3</sub>, which is consistent with observations from plant trials.<sup>13</sup> Based on a black liquor composition of 35.0 wt% C, 35.4 wt% O, 19.4 wt% Na, 4.2 wt% S, and 3.5 wt% H, the phases formed and the

**Table I.** Typical Compositions (wt%) of Black Liquor from North American Woods<sup>20</sup>

	Softwood		Hardwood	
	Typical	Range	Typical	Range
Carbon	35.0	32–37.5	34.0	31–36.5
Hydrogen	3.5	3.4–4.3	3.4	2.9–3.8
Nitrogen	0.1	0.06–0.12	0.2	0.14–0.2
Oxygen	35.4	32–38	35.0	33–39
Sodium	19.4	17.3–22.4	20.0	18–23
Potassium	1.6	0.3–3.7	2.0	1–4.7
Sulfur	4.2	2.9–5.2	4.3	3.2–5.2
Chlorine	0.6	0.1–3.3	0.6	0.1–3.3
Inert	0.2	0.1–2.0	0.5	0.1–2.0
Total	100.0		100.0	

**Table II.** The Chemical Constituents of Black Liquor Smelt Along with the Composition Range Expected Based on the Composition of North American Woods

Smelt constituent	Na <sub>2</sub> CO <sub>3</sub>	Na <sub>2</sub> S	K <sub>2</sub> CO <sub>3</sub>
Composition range (wt%)	70–75	20–25	2–5
Assumed composition (wt%)	75	25	0
Melting point (°C)	858	1172	901

composition ranges for the resulting smelt are given in Table II along with the melting temperature of each of the components.

The thermodynamic analysis assumed that black liquor was combusted with a stoichiometric amount of oxygen. One of the consequences of this assumption is that the smelt contains Na<sub>2</sub>S whereas Na<sub>2</sub>SO<sub>4</sub> formation would be predicted if an excess of oxygen were present. Although no data are available on the oxygen content in existing black liquor gasifiers, X-ray diffraction (XRD) analysis of the smelt produced in the high-temperature gasifier in New Bern, NC, verified that the smelt was primarily composed of Na<sub>2</sub>CO<sub>3</sub> and Na<sub>2</sub>S. A trace amount of a third phase was detected in the New Bern smelt, but could not be positively identified because of an insufficient number of non-overlapped peaks that had a signal-to-noise ratio greater than the background.

The assumed operating temperature of the gasifier, 950°C, is above the melting temperature of both Na<sub>2</sub>CO<sub>3</sub> ( $T_m = 854^\circ\text{C}$ ) and K<sub>2</sub>CO<sub>3</sub> ( $T_m = 891^\circ\text{C}$ ),<sup>22</sup> which, according to the phase diagram and the expected Na<sub>2</sub>CO<sub>3</sub>:K<sub>2</sub>CO<sub>3</sub> ratio, will form a liquid solution above the liquidus temperature ( $T_{\text{liquidus}} \sim 840^\circ\text{C}$  for 95 wt% Na<sub>2</sub>CO<sub>3</sub>, 5 wt% K<sub>2</sub>CO<sub>3</sub>).<sup>23</sup> Likewise, the phase diagram for Na<sub>2</sub>S and Na<sub>2</sub>CO<sub>3</sub> shows that a liquid should form ( $T_{\text{liquidus}} \sim 780^\circ\text{C}$  for 75 wt% Na<sub>2</sub>CO<sub>3</sub>, 25 wt% Na<sub>2</sub>S) under the gasifier conditions for the expected Na<sub>2</sub>CO<sub>3</sub>:Na<sub>2</sub>S ratio.<sup>24</sup> Although a ternary Na<sub>2</sub>CO<sub>3</sub>–Na<sub>2</sub>S–K<sub>2</sub>CO<sub>3</sub> phase diagram is not available, it is safe to assume that the liquidus temperature of the overall composition will be lower than that for either of the two limiting binary systems. Even though the liquid smelt contains Na<sub>2</sub>S and a minor amount of K<sub>2</sub>CO<sub>3</sub>, its properties should be dominated by the major phase, Na<sub>2</sub>CO<sub>3</sub>. In this study, the thermodynamic simulations considered the full smelt composition as well as each component individually.

Phase-pure mullite (3Al<sub>2</sub>O<sub>3</sub>·2SiO<sub>2</sub>) was used to approximate the chemical composition of an aluminosilicate refractory. For contact of mullite and molten black liquor smelt at 950°C, the thermodynamic software predicted the equilibrium phases to be nepheline (NaAlSi<sub>3</sub>O<sub>8</sub>), corundum ( $\alpha$ -Al<sub>2</sub>O<sub>3</sub>), leucite (KAlSi<sub>2</sub>O<sub>6</sub>), and albite (NaAlSi<sub>3</sub>O<sub>6</sub>). A volume expansion of 30% has been measured for this reaction.<sup>25</sup> Based on the volume difference between mullite and the reaction products, any reaction layer would be expected to crack and spall, exposing the underlying material to further attack. The reaction products expected for the reaction of mullite with Na<sub>2</sub>S, K<sub>2</sub>CO<sub>3</sub>, and black liquor smelt are summarized in Table III.

The products predicted for the reaction of black liquor smelt and  $\alpha$ -Al<sub>2</sub>O<sub>3</sub> are  $\beta$ -alumina (Na<sub>2</sub>Al<sub>2</sub>O<sub>19</sub>) and  $\beta$ -alumina (NaAl<sub>9</sub>O<sub>14</sub>). As with the mullite reaction, this reaction also results in a substantial volume increase, 13% in this case.<sup>25</sup> The products predicted for the reaction of  $\alpha$ -Al<sub>2</sub>O<sub>3</sub> and each component of black liquor smelt individually are summarized in Table III. From this thermodynamic analysis, the two materials that have been selected for plant trials, alumina, and aluminosilicate refractories,<sup>5</sup> appear to be poor candidates for use in black liquor gasifiers. An improvement of the design of the refractory lining using at least two layers of aluminosilicates with different physical properties (porosity and thermal conductivity) has been patented to reduce the wear rate.<sup>21</sup> However, thermodynamic analysis indicates that this type of refractory is not a promising candidate for use in alkali environments.

As part of this study, a variety of additional single component ceramics were considered for contact with black liquor including

**Table III. Reaction Products Predicted for Candidate Refractories Exposed to Na<sub>2</sub>CO<sub>3</sub>, K<sub>2</sub>CO<sub>3</sub>, Na<sub>2</sub>S, or Black Liquor Smelt from Thermodynamic Analysis**

Candidate material	Na <sub>2</sub> CO <sub>3</sub>	K <sub>2</sub> CO <sub>3</sub>	Na <sub>2</sub> S	Black liquor smelt
Al <sub>2</sub> O <sub>3</sub>	NaAlO <sub>2</sub>	KAlO <sub>2</sub>	NR	Na <sub>2</sub> Al <sub>12</sub> O <sub>19</sub> , NaAl <sub>9</sub> O <sub>14</sub> , KAl <sub>9</sub> O <sub>14</sub> , slag
3Al <sub>2</sub> O <sub>3</sub> · 2SiO <sub>2</sub>	α-Al <sub>2</sub> O <sub>3</sub> NaAlSiO <sub>4</sub>	α-Al <sub>2</sub> O <sub>3</sub> KAlSiO <sub>4</sub>	NaAlSiO <sub>4</sub> Al <sub>2</sub> O <sub>3</sub> , Al <sub>2</sub> S <sub>3</sub>	NaAlSiO <sub>4</sub> , Al <sub>2</sub> O <sub>3</sub> , KAlSi <sub>2</sub> O <sub>6</sub> , NaAlSi <sub>3</sub> O <sub>8</sub>
CeO <sub>2</sub>	NR	NR	NR	Ce <sub>18</sub> O <sub>31</sub>
ZrO <sub>2</sub>	NR	NR	NR	ZrC <sub>4</sub>
MgO	NR	NR	NR	NR
Y <sub>2</sub> O <sub>3</sub>	NR	NR	NR	NR
MgAl <sub>2</sub> O <sub>4</sub>	MgO NaAlO <sub>2</sub>	MgO KAlO <sub>2</sub>	MgO, Al <sub>2</sub> O <sub>3</sub> ( < 0.1E-05 mol%)	MgO, NaAlO <sub>2</sub> , KAlO <sub>2</sub>
LiAlO <sub>2</sub>	NR	NR	NR	KAlO <sub>2</sub> (< 0.1 wt%)
BaAl <sub>2</sub> O <sub>4</sub>	NR	NR	NR	Ba <sub>3</sub> Al <sub>2</sub> O <sub>6</sub> , KAlO <sub>2</sub>

NR, no reaction.

MgO, CaO, ZrO<sub>2</sub>, Y<sub>2</sub>O<sub>3</sub>, La<sub>2</sub>O<sub>3</sub>, CeO<sub>2</sub>, Li<sub>2</sub>O, BaO, SiC, and Si<sub>3</sub>N<sub>4</sub>. From the simulations that considered these compounds individually, only BaO, SiC, and Si<sub>3</sub>N<sub>4</sub> were predicted to react with the smelt and its components. In contrast to the solid reaction products formed by mullite, α-Al<sub>2</sub>O<sub>3</sub>, and the other oxide ceramics, both SiC and Si<sub>3</sub>N<sub>4</sub> reacted to form compounds such as Na<sub>2</sub>Si<sub>2</sub>O<sub>5</sub> and K<sub>2</sub>Si<sub>4</sub>O<sub>9</sub> that were liquid at the reaction temperature. Thus, SiC and Si<sub>3</sub>N<sub>4</sub> are predicted to react and dissolve into the smelt as it flows through the gasifier. Dissolution of Si<sub>3</sub>N<sub>4</sub> into the smelt was also verified experimentally.<sup>4</sup> Similar to α-Al<sub>2</sub>O<sub>3</sub> and 3Al<sub>2</sub>O<sub>3</sub> · 2SiO<sub>2</sub>, BaO reacts with the smelt to form solid compounds, namely BaS and BaCO<sub>3</sub>.

Among the non-reacting single component oxide candidates; MgO, CaO, and La<sub>2</sub>O<sub>3</sub> were predicted to be resistant to attack by the smelt and its components. However, these compounds are prone to hydration. La<sub>2</sub>O<sub>3</sub> was predicted to be resistant to black liquor smelt, but La<sub>2</sub>O<sub>3</sub> is known to hydrate rapidly. XRD analysis of the sintered sample showed that it was converted to La(OH)<sub>3</sub> after exposure to air at room temperature. Clearly, La<sub>2</sub>O<sub>3</sub> is not an acceptable candidate. Thermodynamic analysis using p(H<sub>2</sub>O) = 1 atm showed that both MgO CaO compounds were resistant to hydration at the steady-state operating temperature of 950°C. For both compounds, the tendency to hydrate increased as temperature decreased. Below 524°C, CaO is predicted to hydrate, while the critical temperature for MgO hydration is 266°C. If water is able to penetrate into the refractories through open porosity, the thermal gradient that exists across the lining would mean that hydration behind the hot face may be an issue. This problem could be overcome by using CaO or MgO as an inert hot face coating on top of a more stable insulating substrate. However, these coatings would still be prone to hydration during any interruption in service such as gasifier shutdowns when the hot face temperature decreased below the critical temperature. Based on the critical temperature for hydration, MgO would appear to be the better choice for this application. This analysis considers only the thermodynamics of the reaction and further kinetic studies would be necessary.

The two component oxides that were considered in the thermodynamic simulations were MgAl<sub>2</sub>O<sub>4</sub>, BaAl<sub>2</sub>O<sub>4</sub>, and LiAlO<sub>2</sub>. All three of these aluminates were predicted to be resistant to attack from Na<sub>2</sub>CO<sub>3</sub>. However, only LiAlO<sub>2</sub> was found to be resistant to attack from K<sub>2</sub>CO<sub>3</sub>. None of the compounds was predicted to be resistant to reaction with overall composition of the black liquor smelt. The reaction products are summarized in Table III. These relations are described in more detail elsewhere.<sup>17</sup>

### III. Experimental Procedure

The experimental portion of the work focused on interactions with Na<sub>2</sub>CO<sub>3</sub> to simplify analysis. Materials that did not react with molten Na<sub>2</sub>CO<sub>3</sub> in the initial set of sessile drop tests along with all of the aluminates were also tested with molten K<sub>2</sub>CO<sub>3</sub>. Interactions with Na<sub>2</sub>S were not used because it melts at

~1200°C,<sup>24</sup> which is far above the operating temperature of the gasifier.

#### (1) Sessile Drop Testing

The contact angle for molten Na<sub>2</sub>CO<sub>3</sub> was measured on candidate refractory materials using standard sessile drop testing in accordance with a previously described setup.<sup>17,18</sup> Several of the candidates investigated by thermodynamic modeling were not selected for sessile drop testing. Specifically, BaO and Li<sub>2</sub>O were eliminated because of environmental issues and La<sub>2</sub>O<sub>3</sub> and CaO were not examined because of their very high susceptibility to hydration. Other candidate ceramics were fabricated as cylindrical pellets ~2 cm in diameter. Al<sub>2</sub>O<sub>3</sub>, CeO<sub>2</sub>, and MgO pellets were fabricated through uniaxial pressing (~65 MPa) of a high-purity powder (Al<sub>2</sub>O<sub>3</sub> and CeO<sub>2</sub> > 99.5%, and MgO > 98%) and sintering at 1600°C. Mullite, Y<sub>2</sub>O<sub>3</sub>, MgAl<sub>2</sub>O<sub>4</sub>, BaAl<sub>2</sub>O<sub>4</sub>, and LiAlO<sub>2</sub> pellets were purchased from Custom Technical Ceramics Inc. and ZrO<sub>2</sub> pellet were purchased from Vesuvius McDanel Inc. The density and percent of open porosity of each of the substrates were measured using Archimedes technique (Table IV). Pellets were mounted, ground, and polished using successively finer abrasives with a minimum abrasive size of 1 μm. A resistance heated horizontal tube furnace equipped with a high-purity mullite tube was used for the reactions. A small quantity (0.2–0.3 g) of Na<sub>2</sub>CO<sub>3</sub> was pressed into a cylindrical pellet ~0.6 cm in diameter and ~0.6 cm high, which was placed on the polished specimen. The specimen and Na<sub>2</sub>CO<sub>3</sub> pellet were then placed in a crucible on a D-tube, inserted into the center of the furnace, and leveled. The ends of the furnace were sealed with gas-tight end caps, which had optical quality fused quartz windows to allow for viewing throughout the experiment. An atmosphere of flowing argon (~200 cm<sup>3</sup>/min) was maintained. The specimen was heated at ~6°C/min to 1000°C and held for 10 h. Specimen temperature was monitored with a type K thermocouple sheathed in an alumina tube that was inserted into the furnace just above the crucible. Once the Na<sub>2</sub>CO<sub>3</sub> was melted, a video camera was used to record images of the molten drop.

**Table IV. Physical Properties of the Substrates Tested in Sessile Drop Testing**

Candidate material	Open porosity (vol.%)	Relative density (%)
Al <sub>2</sub> O <sub>3</sub>	<1	99
3Al <sub>2</sub> O <sub>3</sub> · 2SiO <sub>2</sub>	<2	97
CeO <sub>2</sub>	<2	91
ZrO <sub>2</sub>	~0	~100
MgO	<2	97
Y <sub>2</sub> O <sub>3</sub>	<2	96
MgAl <sub>2</sub> O <sub>4</sub>	4	86
LiAlO <sub>2</sub>	12	88
BaAl <sub>2</sub> O <sub>4</sub>	13	69

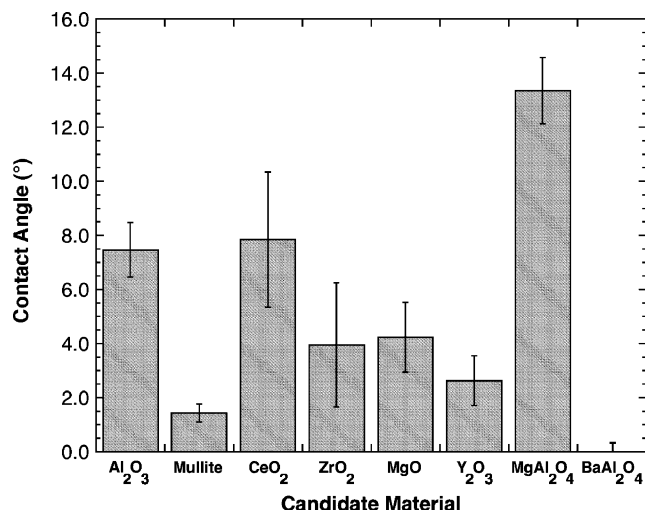


Fig. 2. Contact angle for molten Na<sub>2</sub>CO<sub>3</sub> on candidate refractories. Note: The contact angle was ~0 with a deviation of +0.3 for BaAl<sub>2</sub>O<sub>4</sub>.

Contact angles were measured using images extracted from the video footage. The reported contact angles are the average of five to seven values recorded after the droplet reached a steady-state contact angle.

## (2) Characterization

After sessile drop testing, specimens were examined using grazing incidence XRD (GXRD; X'Pert MRD, Panalytical, Almelo, the Netherlands) to determine the reaction products. In addition to the sessile drop specimens, some of the reaction chemistries were repeated by mixing Na<sub>2</sub>CO<sub>3</sub> with the appropriate ceramic powder and then reacting under identical conditions (1000°C for 10 h). Powder XRD analysis (XRD; XDS 2000, Scintag, Cupertino, CA) was used to determine the phases present after reaction. After examination by GXRD, sessile drop specimens were mounted in epoxy, sectioned perpendicular to the reaction interface, and polished to 1 μm. Polished cross-sections were examined using scanning electron microscopy (SEM; S-570, Hitachi, Tokyo, Japan) and energy dispersive spectroscopy (EDS; AAT, X-ray Optics, Gainesville, FL). X-ray mapping was used to measure the depth of penetration into the substrate.

## IV. Results and Discussion

### (1) Contact Angle Measurement

Contact angles measured for molten Na<sub>2</sub>CO<sub>3</sub> on the candidate materials are shown in Fig. 2. All of the candidate oxides were wet by Na<sub>2</sub>CO<sub>3</sub> at 1000°C. The highest contact angle was observed on MgAl<sub>2</sub>O<sub>4</sub> (13.3° ± 1.2°) and the lowest on BaAl<sub>2</sub>O<sub>4</sub> (~0°). The molten smelt was expected to wet all of the oxide refractories as the compounds in the smelt including Na<sub>2</sub>CO<sub>3</sub> are highly ionic.<sup>26</sup> Contact angles measured for molten K<sub>2</sub>CO<sub>3</sub> on the candidate materials are shown in Fig. 3. For K<sub>2</sub>CO<sub>3</sub>, MgO showed the highest contact angle of about 9.9° ± 1.5°. The lowest contact angle was observed for BaAl<sub>2</sub>O<sub>4</sub>, which was completely wet by K<sub>2</sub>CO<sub>3</sub> with a contact angle of about zero.

### (2) XRD

The candidate materials could be divided into three main groups based on XRD analysis: (1) materials that did not react; (2) those that reacted to form expansive phases that exposed the underlying material to further attack; and (3) those that quickly formed a dense, protective reaction layer that limited further reaction. The diffraction results are summarized in Table V.

The first group, materials that did not react with either Na<sub>2</sub>CO<sub>3</sub> or K<sub>2</sub>CO<sub>3</sub>, consisted of only MgO and CeO<sub>2</sub>. This is in agreement with the thermodynamic analysis (Table III),

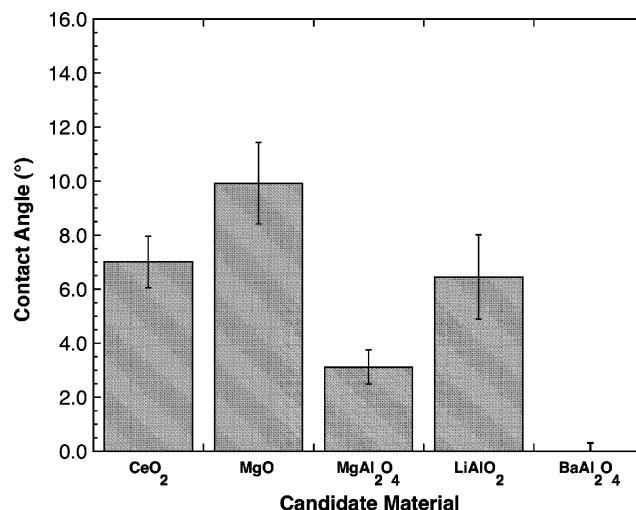


Fig. 3. Contact angle for molten K<sub>2</sub>CO<sub>3</sub> on candidate refractories. Note: The contact angle was ~0 with a deviation of +0.2 for BaAl<sub>2</sub>O<sub>4</sub>.

which did not predict reaction for either of these oxides. Based on relative cost and the commercial availability of MgO bricks, CeO<sub>2</sub>, while resistant to attack, is not currently a viable candidate for high volume industrial production.

The second group that reacted with Na<sub>2</sub>CO<sub>3</sub> to form expansive phases included α-Al<sub>2</sub>O<sub>3</sub>, 3Al<sub>2</sub>O<sub>3</sub> · 2SiO<sub>2</sub>, ZrO<sub>2</sub>, Y<sub>2</sub>O<sub>3</sub>, LiAlO<sub>2</sub>, and BaAl<sub>2</sub>O<sub>4</sub>. After α-Al<sub>2</sub>O<sub>3</sub> was exposed to molten Na<sub>2</sub>CO<sub>3</sub>, NaAlO<sub>2</sub> was found by XRD as had been proposed previously by Hubbard *et al.*<sup>4</sup> A volume expansion of 46% was expected for this reaction based on theoretical density as compared with 30% volume expansion measured by Peascoe *et al.*<sup>25</sup> Mullite reacted with Na<sub>2</sub>CO<sub>3</sub> to form Na<sub>2</sub>Al<sub>2</sub>SiO<sub>6</sub>. The expected volume expansion for this reaction would be 12% based on theoretical density as compared with 13% volume expansion measured by Peascoe *et al.*<sup>25</sup> Similarly, Na<sub>1.75</sub>Al<sub>1.75</sub>Si<sub>0.25</sub>O<sub>4</sub> was formed when mullite contacted with a smelt composed of Na<sub>2</sub>S, Na<sub>2</sub>SO<sub>4</sub>, and Na<sub>2</sub>CO<sub>3</sub>.<sup>4</sup> For contact of Na<sub>2</sub>CO<sub>3</sub> with ZrO<sub>2</sub>, Na<sub>2</sub>ZrO<sub>3</sub> was identified by XRD. Thermodynamic analysis in the current work had predicted no reaction. Earlier work by Yamaguchi<sup>27</sup> did correctly predict the reaction, and his work was verified by XRD analysis in this study. The incorrect prediction of ZrO<sub>2</sub> reactivity in this study, as well as those for Y<sub>2</sub>O<sub>3</sub>, LiAlO<sub>2</sub>, and BaAl<sub>2</sub>O<sub>4</sub>, clearly illustrate the problems that occur when databases contain inaccurate data, or as in this case, no data for certain compounds. In this case, the database employed did not contain data for Na<sub>2</sub>ZrO<sub>3</sub>. For Y<sub>2</sub>O<sub>3</sub>, NaYO<sub>2</sub>, which also did not appear in the database, formed during contact with molten Na<sub>2</sub>CO<sub>3</sub>. The LiAlO<sub>2</sub> specimen cracked during sessile drop testing, probably because of reaction with Na<sub>2</sub>CO<sub>3</sub>. Analysis using GXRD showed that the LiAlO<sub>2</sub> substrate reacted with Na<sub>2</sub>CO<sub>3</sub> to form NaAlO<sub>2</sub>. XRD analysis of the LiAlO<sub>2</sub>

Table V. Products Formed by Reaction of Candidate Refractories with Na<sub>2</sub>CO<sub>3</sub> and K<sub>2</sub>CO<sub>3</sub> at 1000°C as Determined by Sessile Drop Testing Followed by XRD Analysis

Candidate material	Na <sub>2</sub> CO <sub>3</sub>	K <sub>2</sub> CO <sub>3</sub>
Al <sub>2</sub> O <sub>3</sub>	NaAlO <sub>2</sub>	—
3Al <sub>2</sub> O <sub>3</sub> · 2SiO <sub>2</sub>	NaAlSiO <sub>4</sub>	—
CeO <sub>2</sub>	NR	NR
ZrO <sub>2</sub>	Na <sub>2</sub> ZrO <sub>3</sub>	—
MgO	NR	NR
Y <sub>2</sub> O <sub>3</sub>	NaYO <sub>2</sub>	—
MgAl <sub>2</sub> O <sub>4</sub>	MgO, NaAlO <sub>2</sub>	MgO, KAlO <sub>2</sub>
LiAlO <sub>2</sub>	NaAlO <sub>2</sub>	K <sub>6</sub> Al <sub>44</sub> O <sub>69</sub>
BaAl <sub>2</sub> O <sub>4</sub>	NaAlO <sub>2</sub>	Ba <sub>3</sub> Al <sub>2</sub> O <sub>6</sub>

NR, no reaction; —, no experiment.

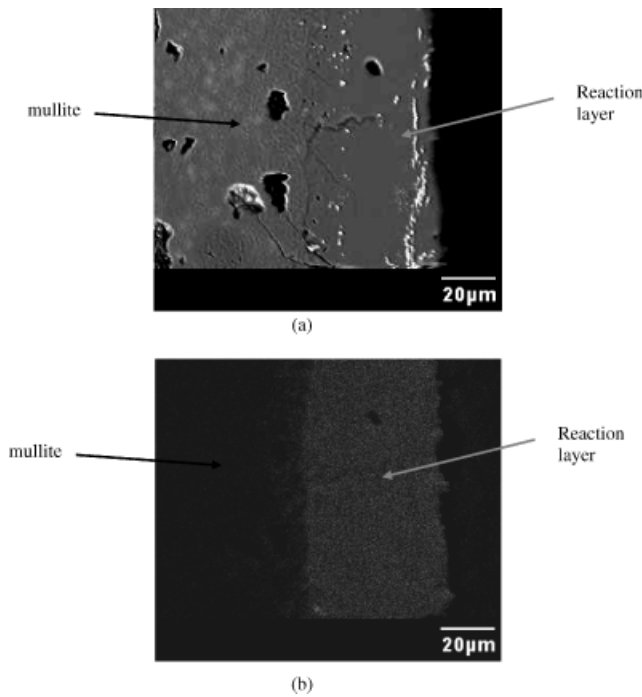


**Fig. 4.** (a) Scanning electron microscopy (SEM) micrograph showing the reaction layer that resulted from molten  $\text{Na}_2\text{CO}_3$  in contact with mullite and (b) an energy dispersive spectroscopy (EDS) map of Na (note that the image and EDS map have different magnifications).

substrate exposed to  $\text{K}_2\text{CO}_3$  showed some peaks that could be attributed to the formation of  $\text{K}_6\text{Al}_{44}\text{O}_{69}$  or  $\text{KAlO}_2$ , but the peaks could not be assigned unambiguously because of the similarity of the patterns and the signal-to-noise ratio of the data.  $\text{BaAl}_2\text{O}_4$  also reacted with  $\text{Na}_2\text{CO}_3$  and, like the other aluminates that were tested, reacted to form  $\text{NaAlO}_2$ . For the reaction of  $\text{BaAl}_2\text{O}_4$  with  $\text{K}_2\text{CO}_3$ , one of the reaction products was  $\text{Ba}_3\text{Al}_2\text{O}_6$ , unlike the other aluminates that all reacted to form potassium-containing compounds.

It is interesting to note that the formation of a lithium-rich layer on aluminosilicate refractories has been reported as a method to increase resistance to alkali attack.<sup>28,29</sup> In this method, a lithium containing material such as  $\text{LiOH}$  or  $\text{Li}_2\text{CO}_3$  is applied to the refractory surface, which is then heated to a sufficient temperature so that the lithium containing material forms an alkali resistant surface layer. The composition of the surface layer has not been reported in detail. It generally comprises crystalline and/or glassy phases that may include lithium aluminate, lithium silicate, or lithium aluminosilicate depending on the composition of the starting refractory material.<sup>29</sup> Apparently, the different composition of the surface layer as compared with the pure  $\text{LiAlO}_2$  investigated in this study, changes the behavior of refractory material against alkali attack. Other refractory materials such as alumina, mixed  $\alpha$ - $\beta$  alumina, and  $\text{MgAl}_2\text{O}_4$ -based refractories have shown improved resistance to molten alkali salts after a lithium treatment although not to the extent observed for mullite-based refractories.<sup>29</sup> This may indicate that a surface layer containing glassy or crystalline silica could be resistant to alkali attack.

The only oxide that fell into the final group of materials that reacted but formed protective phases was  $\text{MgAl}_2\text{O}_4$ . Upon reaction with  $\text{Na}_2\text{CO}_3$ ,  $\text{MgAl}_2\text{O}_4$  was converted to  $\text{MgO}$  and  $\text{NaAlO}_2$  (Table V), similar to the results reported by Hubbard *et al.*<sup>4</sup> The penetration of the reaction layer into the substrate was minimal ( $< 10 \mu\text{m}$ ) relative to reactions that formed expansive phases, because of the formation of a protective layer of  $\text{MgO}$  (Fig. 6). Likewise,  $\text{MgAl}_2\text{O}_4$  reacted with  $\text{K}_2\text{CO}_3$  to form  $\text{MgO}$  and  $\text{KAlO}_2$  (Table V). As with the reaction with  $\text{Na}_2\text{CO}_3$ ,  $\text{MgO}$  is also presumed to form a protective layer in this system. One possible reaction path that would be consistent with the

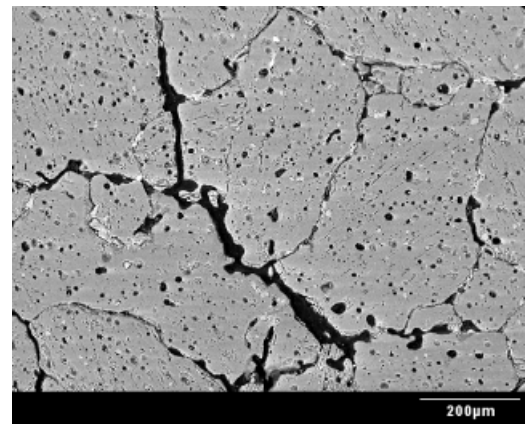


**Fig. 5.** Crack formation of  $\text{LiAlO}_2$  substrate with molten  $\text{Na}_2\text{CO}_3$ .

observed behavior would have  $\text{MgAl}_2\text{O}_4$  dissociate to  $\text{MgO}$  and  $\text{Al}_2\text{O}_3$  first and then the  $\text{Al}_2\text{O}_3$  would react with the carbonates to form alkali aluminates. Once a sufficient quantity of  $\text{MgO}$  forms, it could protect the underlying  $\text{MgAl}_2\text{O}_4$  from further

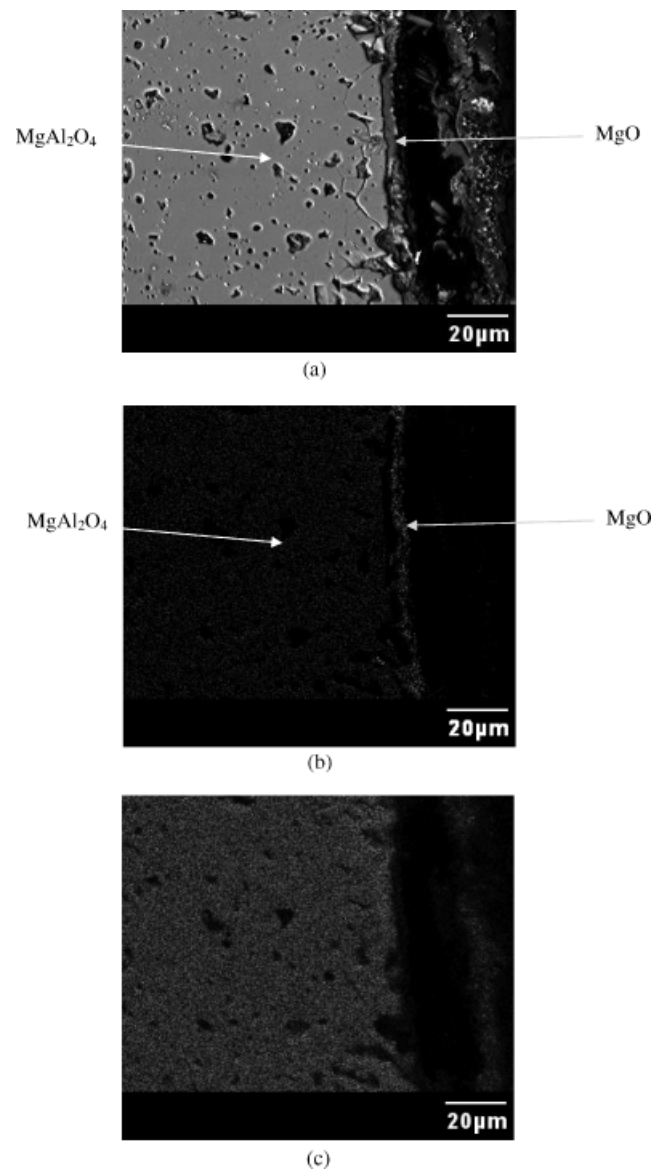


**Fig. 6.** (a) SEM micrograph showing dense  $\text{MgO}$  layer on  $\text{MgAl}_2\text{O}_4$  substrate and energy dispersive spectroscopy mapping showing (b) Mg enrichment, (c) Al depletion from the reaction layer.

reaction. Unlike using MgO refractories that would be susceptible to hydration, MgAl<sub>2</sub>O<sub>4</sub> is stable against hydration and would react with the smelt to form the protective MgO layer. If the MgO layer was damaged in service or by hydration during shut down, the underlying MgAl<sub>2</sub>O<sub>4</sub> would react with the smelt and repair itself *in situ*.

By comparing the results of thermodynamics (Table III) with the results of XRD from sessile drop testing (Table V), it was found that the thermodynamics and experiment were not in agreement for ZrO<sub>2</sub>, Y<sub>2</sub>O<sub>3</sub>, LiAlO<sub>2</sub>, and BaAl<sub>2</sub>O<sub>4</sub>. For α-Al<sub>2</sub>O<sub>3</sub>, thermodynamics predicted the formation of Na<sub>2</sub>Al<sub>12</sub>O<sub>19</sub> (β'-alumina). However the amount of this phase compared with the amount of NaAlO<sub>2</sub> was very small (Na<sub>2</sub>Al<sub>12</sub>O<sub>19</sub>/NaAlO<sub>2</sub> ≈ 1.4 × 10<sup>-5</sup>) to the extent that is not detectable by grazing incidence XRD technique. For mullite, thermodynamics predicted the instability of the candidate in contact with the smelt; but the reaction products predicted by thermodynamics were not completely in agreement with the results of XRD analysis. In contrast to the prediction by thermodynamics, α-Al<sub>2</sub>O<sub>3</sub> was not identified by X-ray but NaAlSiO<sub>4</sub>, which was also predicted by thermodynamics, was identified. Some unidentified peaks were present in the pattern, which could belong to complex compounds in Na–Al–Si–O system. These XRD peaks could be caused by non-equilibrium phases that may disappear if longer reaction times were employed. The other reason for the discrepancy could be the lack of thermodynamic data in the database for one of the compounds, as discussed above. For MgAl<sub>2</sub>O<sub>4</sub>, the correct reaction was predicted by thermodynamics, but the reaction was impeded by the formation of a diffusion barrier (MgO) that inhibited further reaction.

### (3) Penetration

The penetration of Na compounds into candidate refractories was investigated using X-ray mapping of polished cross-sections of sessile drop specimens. As expected, based on thermodynamics and the large volume change associated with the reaction, Na penetrated into mullite forming a distinct reaction layer at the surface of the substrate (Fig. 4). Mapping showed that the reaction layer was about 50 μm thick after sessile drop test. In this geometry, it is likely that the depth of penetration was limited by the quantity of the reactant (Na<sub>2</sub>CO<sub>3</sub>) during the reaction as all of the smelt was consumed. For alumina, the thickness of the reaction layer was about 100 μm. Based on the volume change associated with the reaction, deeper Na penetration would be expected for alumina than mullite.

The reaction layer for the ZrO<sub>2</sub> substrate was thin compared with alumina and mullite, ~5 μm. Analysis by GXRDR verified the formation of Na<sub>2</sub>ZrO<sub>3</sub> as predicted by Yamaguchi.<sup>27</sup> Based on the reported densities, a volume expansion of 46% is predicted for conversion of ZrO<sub>2</sub> to Na<sub>2</sub>ZrO<sub>3</sub>, comparable with the expansions predicted for the reactions of alumina and mullite. Although ZrO<sub>2</sub> reacted with Na<sub>2</sub>CO<sub>3</sub> and formed an expansive phase, the rate of penetration was slow compared with alumina and mullite. The reaction layer for Y<sub>2</sub>O<sub>3</sub> was also relatively thin, ~5–10 μm. Analysis by GXRDR confirmed the formation of NaYO<sub>2</sub>, which should result in a volume expansion of ~15%. Based on sessile drop tests, ZrO<sub>2</sub> and Y<sub>2</sub>O<sub>3</sub> could be candidates for black liquor smelt contact applications because of significantly slower penetration rates compared with alumina and aluminosilicates. However, neither showed the chemical resistance demonstrated by MgO or MgAl<sub>2</sub>O<sub>4</sub>.

Among the aluminates, both the LiAlO<sub>2</sub> and BaAl<sub>2</sub>O<sub>4</sub> substrates contained open porosity. Thus, separation of the effects of penetration because of flow through pores from penetration because of formation of a reaction layer was difficult. As reported in the previous section, Na<sub>2</sub>CO<sub>3</sub> reacted readily with both of these aluminates and significant penetration (on the order of the penetration observed for alumina and mullite) would be expected. As discussed previously, widespread cracking was observed upon reaction of LiAlO<sub>2</sub> with Na<sub>2</sub>CO<sub>3</sub> (Fig. 5). The cracking

appeared to follow the grain boundaries suggesting them as the primary route of attack in this material.

Although Na<sub>2</sub>CO<sub>3</sub> did not react with CeO<sub>2</sub>, some penetration of the smelt through the pores was detected. This penetration is attributed to flow of the smelt through the small volume fraction of open pores, not reaction. Archimedes density measurements found ~2 vol% open porosity in the CeO<sub>2</sub> substrate. Neither thermodynamic analysis nor XRD indicate that CeO<sub>2</sub> should react with Na<sub>2</sub>CO<sub>3</sub>. Thus, CeO<sub>2</sub> should be considered among the candidates for black liquor contact applications, if the price and availability issues are overcome.

Based on thermodynamic analysis and sessile drop studies, dense MgO is resistant to penetration and is a candidate for applications requiring contact with molten black liquor smelt. Although the smelt was found to react with MgAl<sub>2</sub>O<sub>4</sub>, a dense MgO layer was formed *in-situ* (Fig. 6), preventing further attack. The layer was approximately 3–4 μm thick and it appeared to protect the underlying MgAl<sub>2</sub>O<sub>4</sub> substrate from further attack. Based on these results, further testing with MgO or MgAl<sub>2</sub>O<sub>4</sub> as monolithic materials or as coatings on other substrates is warranted.

## V. Summary and Conclusions

The results of thermodynamics and experiment for the reaction of black liquor smelt with various ceramics were in agreement for some candidate materials but not for others. Reactions were correctly predicted for Al<sub>2</sub>O<sub>3</sub>, CeO<sub>2</sub>, MgO, MgAl<sub>2</sub>O<sub>4</sub>, but not for 3Al<sub>2</sub>O<sub>3</sub> · 2SiO<sub>2</sub>, ZrO<sub>2</sub>, Y<sub>2</sub>O<sub>3</sub>, LiAlO<sub>2</sub>, BaAl<sub>2</sub>O<sub>4</sub>. Failure of the thermodynamic predictions was attributed to lack of data for the reaction products produced by reaction of molten black liquor smelt with candidate materials. Sessile drop experiments were used to verify thermodynamic predictions and to determine contact angles of the molten Na<sub>2</sub>CO<sub>3</sub> and K<sub>2</sub>CO<sub>3</sub> on candidate materials. MgAl<sub>2</sub>O<sub>4</sub> showed the highest contact angle with Na<sub>2</sub>CO<sub>3</sub> (13.3° ± 1.2°) while the highest contact angle for K<sub>2</sub>CO<sub>3</sub> (9.9° ± 1.5°) was obtained with MgO. Although CeO<sub>2</sub> and MgO were wet by Na<sub>2</sub>CO<sub>3</sub> and K<sub>2</sub>CO<sub>3</sub>, they did not react with either. Consequently, either CeO<sub>2</sub> or MgO could be used for refractories for applications requiring contact with black liquor smelt. The best choice for this application may be MgAl<sub>2</sub>O<sub>4</sub>. Although MgAl<sub>2</sub>O<sub>4</sub> reacts with both Na<sub>2</sub>CO<sub>3</sub> and K<sub>2</sub>CO<sub>3</sub>, a dense layer of MgO forms quickly and prevents further attack. Based on these considerations, MgO and MgAl<sub>2</sub>O<sub>4</sub> are suggested for further investigation in the form of rotary finger corrosion tests, sessile drop studies with actual black liquor smelt, or trials in test gasifiers.

## References

1. See program description at <http://www.eere.energy.gov>
2. H. F. J. Wenzl, *Kraft Pulping: Theory and Practice*. Lockwood Publishing Company, New York, 1967.
3. M. Agneta, *Kraft Pulping: A Compilation of Notes*. Tappi Press, Atlanta, GA, 1989.
4. C. R. Hubbard, R. A. Peascoe, and J. R. Keiser, "Pulp and Paper Plant Materials Issues Addressed by X-Ray and Neutron Diffraction Methods," *Adv. X-Ray Anal.*, **46**, 278–84 (2003).
5. J. R. Keiser, R. A. Peascoe, C. R. Hubbard, and J. P. Gorog, "Corrosion Issues in Black Liquor Gasifiers"; in *Corrosion/2003 Conference Proceedings*, National Association of Corrosion Engineering, San Diego, CA, March 16–20, 2003.
6. J. Diebold, "Research into the Pyrolysis of Pure Cellulose, Lignin, and Birch Wood Flour in the China Lake Entrained-Flow Reactor"; Report number Ser/TR-332-586, Solar Energy Research Institute, Golden, CO, 1980.
7. P. McKendry, "Energy Production from Biomass (Part 2): Conversion Technologies," *Bioresour. Technol.*, **83** [1] 47–54 (2002).
8. S. Consonni, E. D. Larson, and N. Berglin, "Black Liquor-Gasification/Gas Turbine Cogeneration," *J. Eng. Gas. Turb. Power*, **120** [3] 442–9 (1998).
9. L. Stigsson and B. Hesseborn, "Gasification of Black Liquor"; pp. 277–95 in *International Chemical Recovery Conference Proceedings*, Vol. B, Toronto, ON, April 24–25, 1995, Technical Section CPPA, Montreal, QC, 1995.
10. C. L. Verrill, J. B. Kitto, and J. A. Dickinson, "Development and Evaluation of a Low-Temperature Gasification Process for Chemical Recovery from Kraft Black Liquor"; pp. 1067–78 in *International Chemical Recovery Conference Proceedings*, Tampa, FL, June 1–4, 1998 TAPPI Press, Atlanta, GA, 1998.

- <sup>11</sup>E. Dahlquist and R. Jacobs, "Development of a Dry Black Liquor Gasification Process"; pp. 457–71 in *International Chemical Recovery Conference Proceedings*, Seattle, WA, June 7–11, 1992 TAPPI Press, Atlanta, GA, 1992.
- <sup>12</sup>C. Brown, P. Smith, N. Holmblad, G. M. Christiansen, and B. Hesseborn, "Update of North America's First Commercial Black Liquor Gasification Plant"; pp. 33–49 in *Engineering and Papermakers Conference Proceedings*, Nashville, TN, October 6–9, 1997 TAPPI Press, Atlanta, GA, 1997.
- <sup>13</sup>L. Stigsson, "Chemrec Black Liquor Gasification"; pp. 663–674 in *International Chemical Recovery Conference Proceedings*, Tampa, FL, June 1–4, 1998 TAPPI Press, Atlanta, GA, 1998.
- <sup>14</sup>T. M. Grace and W. M. Timmer, "A Comparison of Alternative Black Liquor Recovery Technologies"; pp. 269–B275 in *International Recovery Conference Proceedings*, Vol. B, Toronto, ON, Canada, April 24–25, 1995, Technical Section CPPA, Montreal, QC, 1995.
- <sup>15</sup>E. D. Larson and D. R. Raymond, "Commercializing Black Liquor and Biomass Gasifier/Gas Turbine Technology," *TAPPI J.*, **80** [2] 50–7 (1997).
- <sup>16</sup>A. R. Rezaie, W. L. Headrick, W. G. Fahrenholtz, R. E. Moore, M. Velez, and W. A. Davis, "Interaction of Refractories and Alkaline Containing Corrodants," *Refractories Applications News*, **9** [5] 26–31 (2004).
- <sup>17</sup>A. R. Rezaie, W. G. Fahrenholtz, and W. L. Headrick, "Thermodynamics of Refractories for Black Liquor Gasification"; pp. 53–62 in *Ceramic Transactions, Vol. 158, Surfaces, Interfaces, and the Science of Ceramic Joining*, Vol. 158, Edited by K. S. Weil, I. E. Reimanis, and C. A. Lewinsohn. The American Ceramic Society, Westerville, OH, 2004.
- <sup>18</sup>A. R. Rezaie, W. L. Headrick, and W. G. Fahrenholtz, "Refractories for Black Liquor Gasification"; pp. 92–103 in *Proceedings of the Tehran International Conference on Refractories*, Tehran, Iran, May 4–6, 2004.
- <sup>19</sup>W. E. Lee and S. Zhang, "Melt Corrosion of Oxide and Oxide-Carbon Refractories," *Int. Mater. Rev.*, **44** [3] 77–104 (1999).
- <sup>20</sup>J. Gullichsen and H. Paulapuro, *Chemical Pulping*. TAPPI Press, Atlanta, GA, 1999.
- <sup>21</sup>B. Nilsson, "Ceramic Insulation in Reactor for Gasification of Residual Products Obtained from Pulp Production"; Int. Patent. No. WO0137984, May 2001.
- <sup>22</sup>*Handbook of Chemistry and Physics*, 62nd Edition, CRC Press, Boca Raton, FL, 1981.
- <sup>23</sup>Diagram number 1008, Phase Diagrams for Ceramists, Vol. I, The American Ceramic Society, Columbus, OH, 1964.
- <sup>24</sup>Diagram number 6165, Phase Diagrams for Ceramists, Vol. V, The American Ceramic Society, Columbus, OH, 1983.
- <sup>25</sup>R. A. Peascoe, J. R. Keiser, C. R. Hubbard, and M. P. Brady, "Performance of Selected Materials in Molten Alkali Salts"; pp. 189–200 in *10th International Symposium on Corrosion in the Pulp and Paper Industry Proceedings*, Helsinki, Finland, August 21–24, 2001. Technical Research Centre of Finland, Espoo, Finland, 2001.
- <sup>26</sup>Stephen C. Carniglia and Gordon L. Barna, *Handbook of Industrial Refractories Technology: Principles Types, Properties, & Applications*. Noyes Publications, Park Ridge, NJ, 1992.
- <sup>27</sup>A. Yamaguchi, "Reactions Between Alkaline Vapors and Refractories for Glass Tank Furnaces"; pp. 1–8 in *10th International Congress on Glass Proceedings*, Edited by M. Kunigi, M. Tashiro, and N. Saga. Ceramic Society of Japan, Kyoto, Japan, 1974.
- <sup>28</sup>J. G. Hemrick, J. R. Keiser, R. A. Peascoe, and C. R. Hubbard, "Refractory Testing and Evaluation at Oak Ridge National Laboratory for Black Liquor Gasifier Applications," *Refract. Appl. News*, **9** [6] 13–20 (2004).
- <sup>29</sup>R. A. Peascoe, C. R. Hubbard, J. R. Keiser, and P. Gorog, "Alkali Resistant Refractories"; U.S. Patent. No. US20050037226A1, February 17, 2005. □